Surface and Bulk Measurements of Metals Deposited on Activated Carbon

Sang Hyun Park,[†] Skye McClain,[†,‡] Zheng Rong Tian,[†] Steven L. Suib,*[,†,‡,§] and Christopher Karwacki*[,⊥]

U-60, Department of Chemistry, Institute of Material Science, and Department of Chemical Engineering, University of Connecticut, Storrs, Connecticut 06269-3060, and US Army, ERDEC, SCERD-RTE, Aberdeen Proving Ground, Maryland 21010-5423

Received May 10, 1996. Revised Manuscript Received August 8, 1996[⊗]

Diffuse reflectance Fourier transform infrared spectroscopy, X-ray photoelectron spectroscopy, scanning Auger microscopy, elemental analyses, BET surface area, and thermogravimetric analyses have been used to study metals and adsorbed organics on the surface of metal-loaded activated carbon materials. Metals such as copper, zinc, and molybdenum have been deposited on activated carbon via incipient wetness methods. Studies of ground and unground samples show that the organic functional groups such as OH, CH_2, CH_3, C═O, C−O, C−O−C, and CH are exclusively found on the exterior of the metal loaded samples and not in the bulk. Surface studies show that Cu and Zn deposits are on the surface whereas Mo is deposited throughout the bulk of the Mo-loaded activated carbon systems. Surface data for the Cu system suggest the presence of $CuCO_3$ and $Cu(OH)_2$. The Zn species appears to be Zn^{2+} on the basis of XPS and SAM data. Mo appears to be oxidized, but a specific oxidation state and the oxidic species are not yet able to be determined.

Introduction

Plain activated and metal-impregnated activated carbons are good materials for the adsorption of hydrocarbons, halogenated hydrocarbons, alcohols, phosgene, hydrogen cyanide, cyanogen chloride, and other materials. One of the major areas of research with activated carbon involves use of Fourier transform infrared spectroscopy to study the nature of functional groups in such materials.[1−21] Several types of functional groups have been reported to exist on the surface of activated carbon, but oxygen and hydrogen derivatives are predominant. The variation of compositions in external and internal areas is possible.[22] In many studies of activated carbon with FTIR, the functional group composition of external and internal areas as well as organic and inorganic impurities in activated metal impregnated carbons are very important due to specific characteristics of these materials and due to interactions of these materials with moisture.

Metal-loaded activated carbon samples are currently under investigation in our laboratories. These materials are of interest as adsorbents of toxic species.[23−27] In many cases, multiple metals are deposited on activated carbons in these systems. The nature of the oxidation states and identity of surface metal species have been studied. However, it is not exactly clear how the metals interact with the surface and how different synthesis conditions can alter the nature of resulting surface species.

The research reported here addresses the nature of surface metal and organic species that are generated

[†] Department of Chemistry.
[‡] Institute of Material Science.
[§] Department of Chemical Engineering.
[⊥] US Army.
* To whom correspondence should be addressed.
[⊗] Abstract published in *Advance ACS Abstracts,* October 1, 1996.

(1) Venter, J. J.; Vannice, M. A. *Carbon* **1988**, *26*, 889−902.
(2) Van Every, K. W.; Griffiths, P. R. *Appl. Spectrosc.* **1991**, *45*, 347−359.
(3) Fanning, P. E.; Vannice, M. A. *Carbon* **1993**, *31*, 721−730.
(4) O'Reilly, J. M.; Mosher, R. A. *Carbon* **1983**, *21*, 47−51.
(5) Meldrum, B. J.; Rochester, C. H.; *J. Chem. Soc., Faraday Trans.* **1983**, *86*, 1881−1884.
(6) Silvertein, R. M.; Bassler, G. C.; Morrill, T. C. *Spectrometric Identification of Organic Compounds*: John Wiley & Sons: New York, 1991.
(7) Meldrum, B. J.; Rochester, C. H. *J. Chem. Soc., Faraday Trans.* **1991**, *86*, 861−865.
(8) Ishizaki, C.; Marti, I. *Carbon* **1981**, *19*, 409−412.
(9) Socrates, G. *Infrared Characteristic Group Frequencies*; John Wiley & Sons: Chichester, 1980.
(10) Painter, P. C.; Snyder, R. W.; Starsinic, M.; Coleman, M. M.; Kuehn, D. W.; Davis, A. *Appl. Spectrosc.* **1981**, *35*, 475−485.
(11) Prest, Jr. W. M.; Mosher, R. A. *ACS Symp. Ser.* **1982**, *200*, 225−247.
(12) Morterra, C.; Low, M. J. D.; Severdia, A. G. *Carbon* **1984**, *22*, 5−12.
(13) Starsinic, M.; Taylor, R. L.; Walker, Jr. P. L.; Painter, P. C. *Carbon* **1983**, *21*, 69−74.
(14) Zawadzki, J. *Carbon* **1981**, *19*, 19−25.
(15) Meldrum, B. J.; Rochester, C. H. *J. Chem. Soc., Faraday Trans.* **1990**, *86*, 2997−3002.
(16) Friedel, R. A.; Hofer, L. J. E. *J. Phys. Chem.* **1970**, *74*, 2921−2922.
(17) Bradbury, A. G. W.; Shafizadeh, F. *Carbon* **1980**, *18*, 109−116.
(18) Morterra, C.; Low, M. J. D. *Carbon* **1983**, *21*, 283−288.
(19) Meldrum, B. J.; Rochester, C. H. *J. Chem. Soc. Faraday Trans.* **1990**, *86*, 3647−3652.
(20) Zawadzki, J. *Carbon* **1978**, *16*, 491−497.
(21) Papirer, E.; Guyon, E.; Perol, N. *Carbon* **1978**, *16*, 133−140.
(22) Leon Y Leon, C. A.; Sloar, J. M.; Calemma, V.; Radovic, L. R. *Carbon* **1992**, *30*, 797−811.
(23) Rossin, J. A.; Morrison, R. W.; Karwacki, C. J. U.S. Army Chemical Research, Development and Engineering Center Scientific Conference on Chemical Defense Research, Nov 1991, Aberdeen Proving Ground, MD.
(24) Zhiqiang, L.; Mingrong, Z; Kuixue, C. *Carbon* **1993**, *31*, 1179−1184.
(25) Rossin, J. A. *Carbon* **1989**, *27*, 611−613.
(26) Rossin, J. A.; Morrison, R. W. *Carbon* **1993**, *31*, 657−659.
(27) McClain, S.; Park, S. H.; Tian, Z. R.; Willis, W. S.; Suib, S. L.; Karwacki, C. J. U.S. Army Chemical Research, Development and Engineering Center Scientific Conference on Chemical Deference Research Nov **1993**, Aberdeen Proving Ground, MD.

S0897-4756(96)00271-2 CCC: $14.00

during synthesis of metal loaded activated carbon samples. In this case, only singly loaded metal systems have been studied. We report here the nature of external and internal species as measured by a variety of spectroscopic methods such as diffuse reflectance infrared Fourier transform (DRIFT) spectroscopy, X-ray photoelectron spectroscopy (XPS), scanning Auger microscopy (SAM), elemental analyses, BET surface area, and thermogravimetric analyses (TGA). Both unground and ground materials have been investigated in order to distinguish the species of external and internal areas and differences that might occur among the different metal (Cu, Zn, Mo) systems.

Experimental Section

Materials. Plain activated carbon and 5% Cu, 5% Zn, and 3% Mo impregnated activated carbon samples obtained from US ERDEC were used. $CuCO_3$ and $ZnCO_3$ used for metal impregnation were also obtained from US ERDEC and were analyzed for XPS and SAM studies without further treatment. For DRIFT study, ground KBr (Fisher Scientific Co., IR grade) was used for background collection after heating at 130 °C for 2 h.

XPS. A Leybold Heraeus Model LHS 10 spectrometer with an EA 10 hemispherical analyzer detector and with Al Kα X-ray radiation was used. The calibration of the spectrometer was done using the Au $4f_{7/2}$ transition at 83.98 eV. All samples were introduced into the analysis chamber as granules on an Al holder. A pass energy of 150 eV was used for elemental analysis.

Deconvolution was carried out with a nonlinear least-squares curve-fitting program with a combined (usually 30% Gaussian) Gaussian/Lorentzian function.[28] The carbon 1s transition for polyaromatic material, whose binding energy is 284.6 eV, was used for charge correction after deconvolution. The peak area sensitivity factor method for quantitative analysis was used. During data collection the pressure in the analysis chamber was maintained in the range of 5×10^{-10} Torr.

SAM. A Perkin-Elmer PHI Model 610 scanning Auger microprobe (SAM) with a cylindrical mirror analyzer was used for surface elemental analysis to a depth of 50 Å, for untreated and crushed granules. An electron beam voltage of 3 kV as a primary beam energy and a low sample current of 20 nA were used for minimizing surface charge accumulation on the sample. Generally a high sample angle, 45−50°, relative to the primary electron beam was used for detection. Granule samples were mounted on In foil for surface analysis up to about 50 Å. For analysis of the interior of granules, the samples were slowly pressed into the In foil with pliers that had been washed with 1-propanol. The internal part (exposed interior) after removing the outer part of the granule was pressed into In foil and loaded into the spectrometer.

Diffuse Reflectance IR. A Nicolet Magna-IR System 750 capable of resolution up to 0.125 cm^{-1} was used. A KBr beamsplitter for the mid-IR range and a MCT (mercury−cadmium−telluride) detector for sensitive detection were used. For diffuse reflectance IR experiments, a special beam collector with a controlled environmental chamber for heating the samples (Spectra Tech Inc., Shelton, CT 06484) fixed on a plate for consistent experimental conditions was used. For stabilization, the MCT detector was cooled with liquid nitrogen for about 2 h prior to data collection. A relatively small aperture angle of 40° out of 150° was used for accuracy and to prevent IR energy saturation of the detector.

The instrument was always purged with nitrogen gas from a liquid nitrogen tank at a flow rate of about 450 mL/min through $^3/_8$ in. Teflon tubing. The samples were preheated at 60 °C for 60 min in the in situ chamber of the instrument to remove residual water. For further drying, the samples were further heated at 130 °C for several hours. The samples were ground slowly with a mortar and a pestle. The background of the spectrometer before data collection was checked with the maximum and minimum intensities at zero path difference (ZPD) of the interferogram. Generally, there were about 2000 scan numbers for all spectra with a resolution of 4 cm^{-1}.

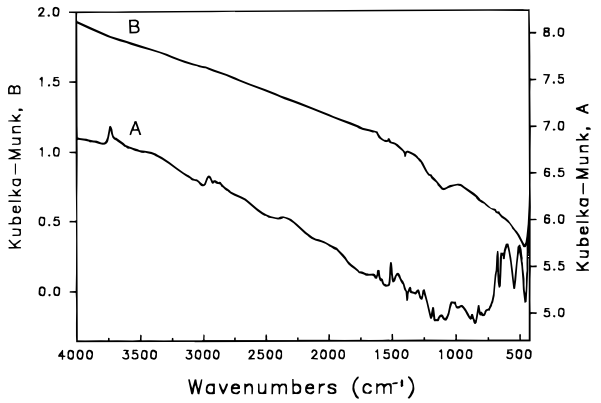

Figure 1. Comparison of DRIFT spectra of activated carbons: (A) granule, (B) ground.

BET. The surface areas of activated carbons were measured at −196 °C by gravimetric methods with a Cahn C2000 vacuum microbalance with a 0.2 μg sensitivity and an MKS baratron pressure measuring unit. The samples were preheated at 110 °C for 5 h for outgassing and left under vacuum conditions to cool to room temperature before measurement. N_2 gas was used as the adsorbate.

Elemental Analysis. For metal analysis, each metal-impregnated sample of 0.25 mg was calcined at 500 °C for 5 h. The residual material was dissolved into the solution containing 20 mL of concentrated nitric acid and 10 mL of concentrated hydrochloric acid. The total volume was adjusted to 100 mL with 30 mL of 0.5 M ammonium chloride and distilled deionized water (DDW). A Perkin-Elmer Plasma 40 emission spectrometer, an inductively coupled plasma-atomic emission spectrometer (ICP-AES), equipped with a transversely mounted pneumatic crossflow nebulizer and a photoelectron multiplier tube, was used for elemental analyses. DDW mixed with the same ratios of nitric acid and ammonium chloride was used for background subtraction in ICP-AES. Standard solutions for calibration were made from 1000 ppm stock solutions (J. T. Baker Inc., Phillipsburg, NJ 08865). Combustion methods with a Perkin-Elmer 2400 CHN elemental analyzer were used for C, H, and N analysis.

Results

Unloaded activated carbon and three single metal-impregnated samples were used for thermal analysis and BET experiments. The weight losses of the samples obtained by thermogravimetric analysis (TGA) up to 150 °C with a temperature programming rate of 1 °C/min under N_2 gas flow (25 mL/min) were about 5% for activated carbon and 2% for metal-impregnated carbons. The surface areas measured by the BET method with N_2 gas were 1129 m^2/g for the neat activated carbon, 1070 m^2/g for Cu (5%) impregnated activated carbon, 1004 m^2/g for Zn (5%) impregnated activated carbon, and 1076 m^2/g for Mo (3%) impregnated activated carbon. All four BET data showed linear correlation coefficients of 0.999 or greater. All four samples showed a typical Type I adsorption isotherm with N_2 gas.

DRIFT spectra for activated carbon granules and ground activated carbon samples are shown in Figure 1A,B, respectively. The relative intensities of the IR peaks of the granules before grinding are nearly 8 times

(28) Sherwood, P .M. A. In *Practical surface analysis by Auger and X-ray photoelectron Spectroscopy*; Briggs, D.; Seah, M. P., Eds.; John Wiley & Sons: London, 1983; appendix 3, p 445.

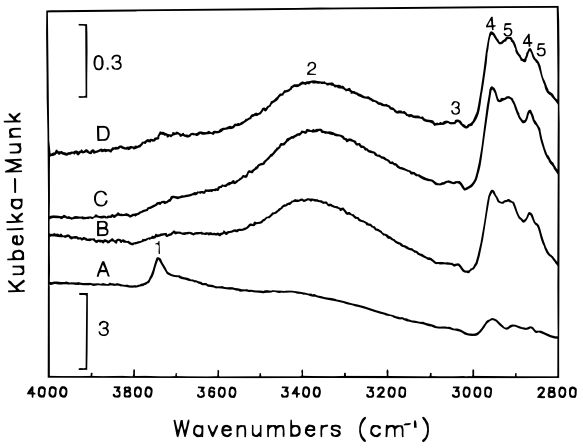

Figure 2. DRIFT spectra in the 4000−2800 cm^{-1} region: (A) activated carbon, (B) activated carbon from different batch, (C) activated carbon with Cu (5%), (D) activated carbon with Mo (3%).

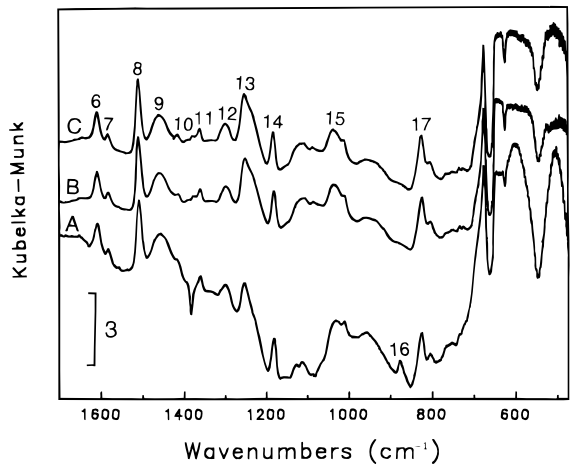

Figure 3. DRIFT spectra in the 1700−470 cm^{-1} region: (A) activated carbon, (B) activated carbon with Cu (5%), (C) activated carbon with Mo (3%).

larger than after grinding over the 4000−500 cm^{-1} range.

Similar data are shown over the range of 4000−2800 cm^{-1} for a series of activated carbon samples in Figure 2. The bar at the bottom is the *Y*-axis scale for spectrum A and the bar in the upper corner is for spectra B−D. Figure 2A,B are DRIFT spectra for two different activated carbon samples. Spectrum A has a better signal-to-noise ratio than spectra B−D and shows a peak near 3730 cm^{-1}. There is also a weak broad band centered near 3390 cm^{-1} in spectrum A. Spectrum B shows a very broad intense peak centered at 3370 cm^{-1}. Figure 2C shows a DRIFT spectrum for activated carbon with 5% Cu, with bands very similar to that of spectrum B (Figure 2B). Figure 2D shows a DRIFT spectrum for activated carbon with 3% Mo, which again is very similar to data of Figure 2B,C.

Figure 3 shows three DRIFT spectra for activated carbon, 5% Cu on activated carbon, and 3% Mo on activated carbon. In the range of 1700−500 cm^{-1}, there are many peaks centered at 1609, 1600,1583, 1510, 1461, 1415, 1379, 1362, 1253, 1126, 1115, 1108, 1038, 878, and 827 cm^{-1}.

After metal impregnation, there is an increase in intensity at 1415 cm^{-1} and a new peak with weak intensity at 1379 cm^{-1}. In the range 1400−1200 cm^{-1}, it is difficult to explain increases or decreases in absorption due to poor correlation between the spectrum (Figure 3A) of activated carbon and the spectra (Figure 3B,C) of metal-impregnated samples. For example, there are two peaks centered at 1115 and 1126 cm^{-1} with activated carbon, but with the metal-impregnated samples, the two peaks merged at 1108 cm^{-1} and the IR intensities decreased. The peak at 878 cm^{-1} in Figure 3A disappeared in Figure 3B,C.

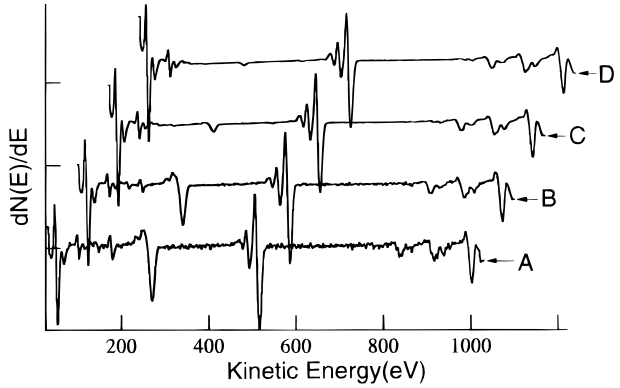

Figure 4. Damage effect on $ZnCO_3$ during continuous Auger analyses: (A) 4 min, (B) 20 min (C) 6 h, (D) 15 h.

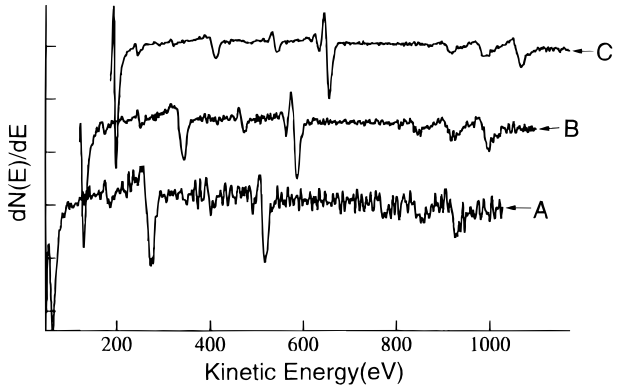

Figure 5. Damage effect on $CuCO_3$ during continuous Auger analyses: (A) 5 min, (B) 40 min, (C) 6 h.

Figure 4 shows scanning Auger microscopy data for $ZnCO_3$ with continuous analysis at a spot. Relative intensities of a series of the peaks at a kinetic energy of 272 eV decrease as analysis time increases from 4 min (Figure 4A) to 20 min (Figure 4B) to 6 h (Figure 4C) to 15 h (Figure 4D). Relative intensities of all other peaks appear to remain the same. There are a series of three peaks in each spectrum at 838, 915, and 1003 eV for Zn. The peak at 515 eV is for oxygen.

Similar trends are shown in Figure 5 after 6 h of continuous analysis. There is a decrease of peak intensity at 272 eV, and the rest of the peaks (407, 515, 775, 846, and 924 eV) remain the same during analysis from 4 min (Figure 5A) to 40 min (Figure 5B) to 6 h (Figure 5C). The peak at 407 eV is due to In, which was used for loading the $CuCO_3$ sample. Figures 4A and 5A have smaller signal-to-noise ratios than other spectra due to the lower scan numbers used for these analyses.

XPS data for Cu-impregnated activated carbon and Zn-impregnated activated carbon in the C 1s region are shown in Figures 6 and 7, respectively. Deconvolution of these data will be described in the Discussion.

Table 2 shows results of SAM analyses with activated carbon and three single metal-impregnated samples. Cu

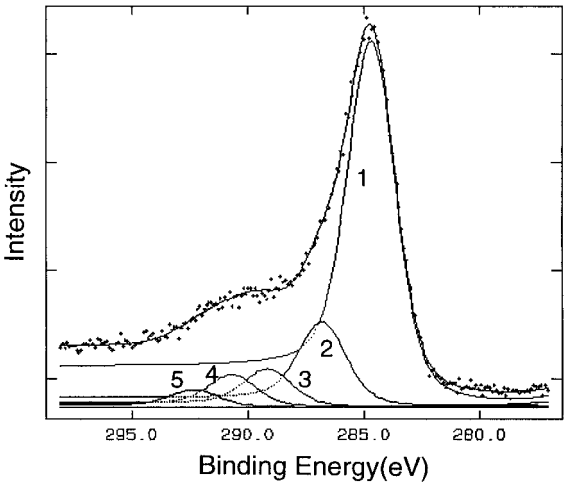

Figure 6. Deconvoluted XPS spectrum of Cu impregnated activated carbon in the C 1s region.

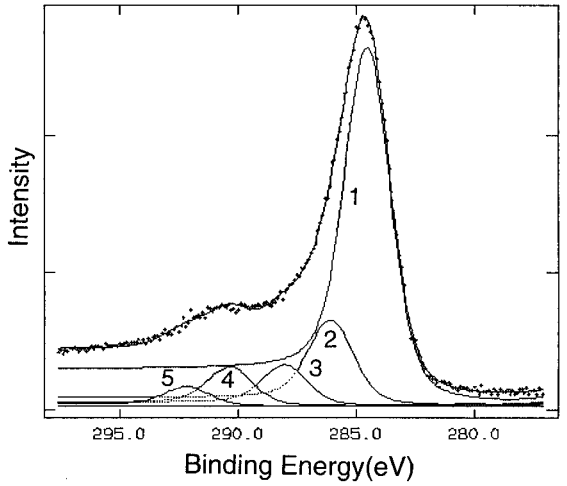

Figure 7. Deconvoluted XPS spectrum of Zn-impregnated activated carbon in the C 1s region.

and Zn exist more on the surface than in the interior. Mo data taken in different spots and depths show low or undetectable Mo concentrations. Oxygen in neat activated carbon as well as in single metal-impregnated activated carbons shows higher concentrations on the surface than the interior surfaces exposed by crushing the granules. Local concentrations of sulfur are similar for uncrushed and crushed samples. Zinc and chloride are also observed on the surface of the Cu-impregnated sample.

Table 3 shows metal/carbon ratios for the three single metal-impregnated samples and results of Rossin et al.[25,26] The metal/carbon ratios given in parentheses are based on elemental analyses. Table 4 shows oxygen/metal ratios on the surface as determined by XPS and SAM methods. Oxygen/metal ratios on the surface determined by XPS are much larger than those by SAM analyses.

Elemental analysis of metal-impregnated samples by ICP-AES is shown in Table 5. Metal concentrations in the samples analyzed by ICP-AES appear to be lower than original loadings. Carbon content in the unloaded sample is shown higher than those in the metal-loaded samples. Small amounts of hydrogen and nitrogen are detected in all samples. Small amounts of Zn are detected in the Cu-loaded sample. Table 5 also contains elements such as O and S which are not detected by elemental analysis method but are known to be present from SAM and XPS experiments.

Discussion

BET and Thermal Analyses. A large surface area is a basic requirement for use of activated carbon as an adsorbent to remove toxic gases such as hydrogen cyanide and cyanogen chloride. It is important to know if there are any changes in surface area or in the structure related to adsorption properties after metal impregnation.

TGA analysis shows that adsorption properties of activated carbons change after metal impregnation. From the results of BET methods and adsorption isotherms, there are only small differences in surface areas after metal impregnation; only a 10% reduction. Some of the mesopores of the structure and some of the surface for nitrogen gas adsorption were blocked after metal impregnation. TGA results show more weight loss with untreated activated carbon and less weight loss with metal impregnated activated carbons, which is consistent with BET data.

Effects of Grinding. Properties such as functionality and hydrophilicity (or hydrophobicity) of the internal (crushed samples) and external surfaces (noncrushed samples) are crucial for controlling the nature of activated carbons. IR spectroscopy is a powerful technique for identifying functional groups in samples. Transmittance IR is not a successful technique for the study of functional groups on activated carbons because of the large light absorption by carbon. Diffuse reflectance IR methods have recently been frequently used for activated carbon[1−3] due to several advantages such as the ability to study highly opaque, weak, or highly IR-absorbing materials; high sensitivity; and minimal sample preparation. One way to study differences between internal and external surface structures is to compare spectra collected by the diffuse reflectance IR technique before and after grinding granules of activated carbon.

From elemental SAM studies (Table 2, Figures 4 and 5), it is clear that the concentration of oxygen on the surface of the granules is generally much higher than that of the interior (after crushing) of the particles. Sulfur on the other hand seems to be evenly distributed in the raw materials before activation on the basis of XPS and SAM data. Figure 1 shows the effect of grinding activated carbon. The functional groups on the surface of the granules after grinding are diluted and show weaker signals than before grinding. The peaks in Figure 1B for the ground granules are very weak, but the wavenumbers of the peaks are the same as those in Figure 1A (activated carbon before grinding).

Particle sizes determined with a scanning electron microscope ranged from 50 μm to about 1 μm after grinding and 0.5−2 mm before grinding. Peak sharpening effects[29] without loss of peak intensity with a continuous change of particle size from diameters larger than 90 μm to smaller than 10 μm was not observed in our study. In the wavenumber range 470−700 cm^{-1}, a couple of irregular strong peaks seem to be due to decreased signal-to-noise ratios.

(29) Fuller, M. P.; Griffiths, P. R. *Anal. Chem.* **1978**, *50*, 1906−1910.

Table 1. Functional Group Assignments on Activated Carbon

peak no.[a]	peak(cm^{-1})	assignment	ref
1	3730	free O−H	4−6, 10, 12
2	3450−3100	hydrogen-bonded O−H, absorbed H_2O	4, 5, 7−9
3	3060, 3035	C−H str in alkene	6, 11
4	2958, 2870	asym and sym str of $-CH_3$	6, 9, 10, 11
5	2920, 2850	asym and sym stretch of $-CH_2-$	6, 10, 11
6	1609	highly conjugated C═O str	4, 7, 24
		C═C str in aromatic system	4, 8, 12−16
7	1583	C═C stretch	3, 7, 8, 14, 15
8	1510	highly red-shifted C═C(?)	3
9	1461, 1415	C−O str in carboxylic group	1, 4, 5, 7−9
10	1379	carboxyl−carbonate or carboxylic salt or metal carbonate	3, 16
11	1361	in-plane bending of O−H	6, 11
12	1300	b	
13	1253	C−O str in cyclic ether attached to double bonds or C−O asym str in ether bridged group	4, 5, 7, 9, 15−21
14	1183	C−O str of carboxylate	1, 4−8
		C−O str of ether	4−7, 9, 18−21
		O−H bending in −COOH	4−8, 11
15	1038	C−O str in alcohol	3, 6, 7, 9
		C−O−C sym str	6, 11, 18
16	878	b	
17	827	out-of-plane bending of C−H in aromatic structure	6, 11

[a] Assignments of peaks in Figures 2 and 3. [b] Not assigned.

Table 2. Atomic Analysis of Activated Carbons by SAM

		weight percent						
samples	analysis condition	C	O	S	Cl	Cu	Zn	Mo
A.C.	internal	96.78	2.01	1.21				
	surface	94.99	3.65	1.36				
		96.28	2.70	1.02				
A.C. w/Cu (5%)	internal	88.41	1.75	2.01		7.83	*a*	
	surface	66.78	7.15	1.24	1.14	23.69	*a*	
		45.89	8.84	0.95	2.16	25.49	16.67	
A.C. w/Zn (5%)	internal	93.42	1.40	1.53			3.65	
	surface	84.36	3.40	1.05			11.19	
		88.33	1.99	2.16			7.52	
A.C. w/Mo (3%)	internal	94.39	1.65	1.88				2.08
	surface	94.89	3.46	1.65				*b*
		94.16	3.96	1.88				*b*

[a] No data. [b] Below detection limit.

Table 3. Atomic Ratio of Metal/Carbon on Activated Carbon by XPS (Elemental Analysis)

sample	Cu/C	Zn/C	Mo/C
AC w/ Cu	0.096 (0.0092)		
AC w/ Zn		0.037 (0.01)	
AC w/ Mo			0.0035 (0.0039)
ASZ[a]	0.022 (0.013)	0.20 (0.012)	
ASZM[a]	0.01 (0.011)	0.16 (0.010)	0.001 (0.003)
ASC−TEDA[b]	0.035 (0.019)[c]		
	0.022 (0.019)[d]		
ASC[b]	0.061 (0.020)[c]		
	0.028 (0.020)[d]		

[a] Reference 26. [b] Reference 25. [c] Granule sample. [d] Crushed sample.

Table 4. Comparison of Oxygen Metal on the Surface by XPS and SAM

	A.C. w/ Cu	A.C. w/ Zn	A.C. w/ Mo
XPS	2.52[b]	5.24	19.33
SAM[a]	1.16	1.20	*c*

[a] Averaged value. [b] Zn contained. [c] No Mo detected.

Comparison of IR Data. After metal impregnation onto activated carbon, chemisorptive properties have been improved. Considerable research on activated carbon by transmittance and diffuse reflectance IR techniques has been done.[1−21] More research needs to be done with metal-impregnated activated carbons. Functional group changes after metal impregnation may lead to a better understanding of the role of impregnated metals in adsorption. The assignments of various functional groups based on FTIR data are given in Table 1.

Table 5. Elemental Analysis of Activated Carbons by ICP−AES and Combustion Method

	weight percent						
samples	C	H	N	Cu	Zn	Mo	balance[a]
A.C.	92.14	0.28	0.50				7.08
A.C. w/ 5% Cu	85.65	0.46	0.97	4.17	.54	*b*	8.21
A.C. w/ 5% Zn	82.77	0.39	0.72	*b*	4.47	*b*	11.65
A.C. w/ 3% Mo	86.35	0.39	0.64	*b*	a	2.72	9.89

[a] S, O, undetected elements. [b] Below detection limit.

In the 4000−2800 cm^{-1} region of Figure 2 with activated carbon and metal impregnated samples, peaks in the 3600−3750 cm^{-1} range are due to stretching of free O−H groups on the surface.[4−6,10] Hydrogen-bonded OH groups can be assigned to the broad peak in the 3350−3390 cm^{-1} range.[5,7,8] From elemental analyses of the surface by SAM (Table 2), there are significant differences in oxygen distributions from spot to spot ranging about from 2% to 11%. The peaks of the functional groups (C−H and O−H) on the samples in the 4000−2800 cm^{-1} region are consistent with hydrogen detection from elemental analyses (Table 5).

FTIR spectra for curves A and B in Figure 2 show the heterogeneous nature of such surfaces in terms of

differences in functional group concentrations for different batches of the same material. The broad peak (Figure 2B) around 3300−3400 cm^{-1} is likely due to adsorbed H_2O after heating at 60 °C because this peak is reduced after additional drying at 130 °C for 12 h as observed in our and in other research.[4] There are also two broad peaks with maxima at 3035 and 3060 cm^{-1} (Figures 2A−D) which are assigned to C−H stretches of alkenes associated with polyaromatic rings.[6] Spectrum A in Figure 2 shows less intense peaks in this range and in the 2800−3000 cm^{-1} region which is due to C−H stretching modes.

Four bands at 2850, 2870, 2920, and 2958 cm^{-1} for untreated activated carbon (Figures 2A,B) and for metal-treated samples (Figure 2C,D) respectively, reveal that all samples contain alkane functionalities. The peaks at 2850 and 2920 cm^{-1} are due to the C−H symmetric and asymmetric stretches of residual methylene groups on the surface and the peaks at 2870 and 2958 cm^{-1} are due to the C−H symmetric and asymmetric stretches of methyl groups.[6,9]

Spectrum A in Figure 3 was obtained for activated carbon and spectra B and C were from the metal-impregnated samples. The peaks at 1609 cm^{-1} observed for all samples are due to highly conjugated C═O stretching vibrations with the aromatic system of activated carbon since such the peaks are observed for other carbon based materials and coals.[4] A C═C stretch in aromatic systems with distorted symmetry due to oxide ligands might also explain peaks near 1600 cm^{-1}.[10−13] Note that the peak intensity near 1600 cm^{-1} did not change after oxidation on heating to 773 K under oxygen.[7] Further discussion of assignments of peaks near 1600 cm^{-1} can be found elsewhere.[4,7,11]

The small peak at 1583 cm^{-1} for all samples of Figure 3 might be due to a C═C stretching mode in the structure[3] or due to increased extinction coefficients for ring systems.[13] The peaks with maxima at 1510 cm^{-1} shown for all samples in Figure 3 can be assigned to C═C moieties which are known to be highly red-shifted on oxygen-rich surfaces[3] or are due to asymmetric stretches of the carboxylic anion.[6]

Two peaks are observed for all activated carbon and metal-loaded samples at 1461 and 1415 cm^{-1} (Figure 3). These peaks are assigned to a C−O stretching vibration of carboxylate groups which are metal dependent and depend on the heating process during metal impregnation. The increased intensity at 1415 cm^{-1} for all three samples of Figure 3 is believed to be related to the presence of metal carbonates.

There is a new peak with weak intensity appearing at 1379 cm^{-1} after metal impregnation as shown in Figure 3B,C. There is increased absorption at 1379 cm^{-1} after neutralization of the carbon surface with $NaHCO_3$, Na_2CO_3, and NaOH solutions. This change may be due to a functional group change from carboxylic acid to the salt form.[14] The increase in peak intensity at 1379 cm^{-1} can also be explained by a carboxylic salt impregnated metal or metal−carbonate interaction (Figure 3B,C). The band at 1362 cm^{-1} is likely due to O−H in-plane bending in aromatic systems (Figure 3A−C).

The intense absorption centered at 1253 cm^{-1} of Figure 3 with a shoulder may be due to cyclic ethers in C−O−C−O−C structures attached to double bonds,[15] or combinations of ether bridging groups,[16,17,19] and non-oxygen-containing groups.[18] A sharp and symmetric peak might be due to one of the possible vibrational modes such as a C−O stretch of the carboxylate groups on the surface of activated carbon (Figure 3A) because the same shape of the peak appeared after metal impregnation (Figure 3B,C). A C−O stretch of ether groups or an (less likely) O−H bending mode of COOH[4] is also a possibility.

After metal impregnation, peaks merge to 1108 cm^{-1} (Figure 3B,C) in the 1140−1100 cm^{-1} region. This effect might be related to ring opening of lactone and cyclic ether C−O bond breakage during the metal-impregnation process.[6,9] The C−O stretching vibration of a terminal alcohol in the residual alkane system whose C−H peaks are shown in the 2850−3000 cm^{-1} range might contribute to the broad peak at 1038 cm^{-1}. A C−O−C symmetric vibrational mode is also consistent with absorption near 2900 cm^{-1}.

Other activated carbon samples gave peaks with different intensities at 878 cm^{-1}, but no absorption with metal-impregnated samples. The 878 cm^{-1} peak is assigned to an out-of-plane C−H bending mode. After metal impregnation, the peak centered at 878 cm^{-1} diminished. The reason for this is uncertain at this time. The peak at 827 cm^{-1} is safely assigned to an out-of-plane C−H bending mode for aromatic systems.[6,9] After metal impregnation, there are changes in peak shape and peak intensity at 1100−1140, 1379, and 1415 cm^{-1} that might be related to metal carbonate and metal salt vibrational modes.

Elemental Analysis. Bulk analyses by ICP-AES methods give 4.17% Cu, 4.47% Zn, and 2.72% Mo in weight percent. These results are substantially different from those obtained by SAM which only provides a semiquantitative analysis at best. In addition, the SAM data are surface sensitive and have contribution only from the top 20−50 Å.

The SAM data of the surface and interior for Cu sample show higher Cu concentration than the ICP-AES data. This implies that the Cu concentration in Cu samples is not uniform. Small amounts of Zn were detected by ICP-AES in the Cu sample, which is consistent with high surface Zn concentration detected by SAM.

A comparison of the SAM and ICP-AES data show that the Zn concentration on the surface is higher than in the bulk. This is also substantiated by SAM data for the internal sample.

The ICP-AES data for the Mo sample show a bulk analysis of 2.72%. This is much larger than that detected by SAM and a little lower than the original loading. In conjunction with SAM analyses shown in Table 2, Mo concentrations in Mo samples may not be uniform.

XPS and SAM. *Metal and Other Elemental Distributions.* Some carbon-based materials such as graphites, carbon fibers, and activated carbons have specific properties such as black color, relative chemical inertness, and polyaromatic structures. Even though significant research on activated carbon has been done, there is still uncertainty in assigning the functional groups on the surface of activated carbons and in explaining the chemical and physical roles of the functional groups especially during sorption of toxic

gases.[23,24] According to recent published research,[23,25,26] some metals such as copper and zinc on the activated carbons exist mainly as metal(II) oxides. Molybdenum exists in several different chemical states.

As shown in Table 2 and in other research,[25] oxygen and metal distributions on the samples are not distributed evenly, as was observed previously.[27] Higher oxygen concentrations on the surface of metal-impregnated activated carbons may be due to metal carbonates moving from the bulk to the external surface during drying after metal impregnation. More oxygen detected on the surface of plain activated carbon can also be explained by easy accessibility of oxygen to the external surface during carbonization and gasification. After crushing the carbon granules to expose new clean carbon surfaces at room temperature, the surface oxygen concentration would be expected to decrease.

Sulfur seems to exist evenly throughout the granules. Reasons the distributions of the two elements (oxygen and sulfur) seem to be different may be due to oxygen introduction during carbonization of raw materials where sulfur might already be present. Therefore, conditions during metal impregnation such as time and temperature for heating and during gasification such as purity of nitrogen or carbon dioxide may be critical for control of hydrophilic functional groups on the surface. The S 2p binding energies from XPS analyses were in the range 164.5 ± 0.3 eV for plain and metal-impregnated activated carbons. Sulfur might exist in carbonaceous environments and not in an acidic or metallic form based on these XPS data. Zinc and chloride impurities are believed to be introduced during the metal-impregnation process.

The metal/carbon ratios determined by XPS and from elemental analyses and Auger data (Table 2) showed similar trends to Rossin et al.[25,26] except in the case of the Mo-impregnated sample. Their and our XPS data are compared in Table 3. The metal-to-carbon ratios on the surface are much higher than theoretical values determined for homogeneously dispersed metal during impregnation. Therefore, metals (except for Mo) primarily exist on the surface rather than in interior sites, as confirmed by our SAM analyses (Table 2). From the combination of SAM data, XPS data, and elemental analyses, Mo appears to be distributed through the granules, but not evenly dispersed. The metal distribution differs for different preparations.

Electron Beam Damage and Metal Carbonate Formation. From Table 4, it is clear that XPS analyses show higher oxygen/metal ratios than SAM. The reason for this may be that sample damage via degasification by the electron beam during Auger analysis may occur. Similarly, damage effects during analysis can occur via ion bombardment of Ar at 3 keV.[30] To study sample damage effects, metal carbonates were used as metal sources for metal impregnation which were mounted in the analysis chamber of the SAM at conditions similar to those used for elemental analyses of activated carbons. Figures 4 and 5 show concentration changes of elements of the $ZnCO_3$ and $CuCO_3$ samples, respectively, during analysis. Unlike the case of $ZnCO_3$ (Figure 4), there was severe charge accumulation on $CuCO_3$ even at a low sample current of 5 nA, which made Auger analyses (Figure 5) difficult and inconsistent. The oxygen/metal ratio on $ZnCO_3$ (homogeneous sample) became close to 1 (1.08 after 5 h). The analysis time for $ZnCO_3$ was shorter than the analysis time for activated carbon samples. In the case of $CuCO_3$ (Figure 5) the oxygen/metal ratio approached 1.33 with continuous analysis at the same spot perhaps due to the heterogeneity of commercial $CuCO_3$ which contains $Cu(OH)_2$. The SAM data for metal carbonates of Figures 4 and 5 are very similar to XPS and Auger data for metal-containing activated carbons.

Carbon Regions and Presence of Metal Carbonates. Peak assignments in the C 1s region after deconvolution have been made for carbon fibers and polymers. After electrochemical oxidation of carbon fibers, deconvolution was used for separating different carbon signals.[31,32] Peak deconvolution of the C 1s region was done.[33] Fluoro-containing compounds were used for chemical modification of functional groups on carbon-based materials[34] and for microplasma treatments on carbon fiber surfaces.[35] Extensive research was done with deconvolution in the C 1s region of Cu- and Zn-impregnated activated carbons for our study (Figures 6 and 7, respectively).

The same full width half-maximum (fwhm), 2.34 eV, was used for all deconvolution in Figures 6 and 7. The main peaks centered at 284.6 eV in Figures 6 and 7 are due to carbon in polyaromatic structures. Peak 2 at 286.6 eV might contain more than one type of carbon since the 285−287.6 eV region represents many functional groups containing oxygen as suggested by IR and XPS studies.[1−21,32−37,40−44] Because of the heterogeneity of the surface, the peaks in Figure 6 (3 at 289.3 eV and 4 at 290.7 eV) may be due to carboxylic salts and metal carbonates.[38,39] The percentage of the two components is near 12.9% (7.0% for peak 3 and 5.9% for peak 4). Assignments of the different peaks of the deconvoluted data of Figures 6 and 7 are consistent with literature data.[31−35]

The ratio of metal (Cu + Zn)/carbon (metal carbonates and metal carboxylates) on activated carbon with copper is 1.2 (11.0/9.4). A ratio larger than 1 may be due to other metal compounds such as metal chlorides and small amounts of metal oxides on the surface. The ratio

(30) Christie, A. B.; Lee, J.; Sutherland, I.; Walls, J. M. *Appl. Surf. Sci.* **1983**, *15*, 224−237.
(31) Harvey, J.; Kozlowski, C.; Sherwood, P. M. A. *J. Mater. Sci.* **1987**, *22*, 1585−1596.
(32) Kozlowski, C.; Sherwood, P. M. A. *Carbon* **1987**, *25*, 751−760.
(33) Bradley, R. H.; Ling, X.; Sutherland, I. *Carbon* **1993**, *31*, 1115−1120.
(34) Takahagi, T.; Ishitani, A. *Carbon* **1988**, *26*, 389−396.
(35) Xie, Y.; Sherwood, P. M. A. *Appl. Spectrosc.* **1989**, *43*, 1153−1158.
(36) Desimoni, E.; Casella, G. I.; Salvi, A. *Carbon* **1992**, *30*, 521−526.
(37) Stoch, J.; Gablankowska-Kukucz, *J. Surf. Interface Anal.* **1991**, *17*, 165−167.
(38) Desimoni, E.; Casella, G. I.; Salvi, A. M.; Catadi, T. R. I.; Morone, A. *Carbon* **1992**, *30*, 527−531.
(39) Morra, M.; Occhiello, E.; Garbassi, F. *Surf. Interface Anal.* **1990**, *16*, 412−417.
(40) Beamson, G.; Briggs, D. *Surf. Interface Anal.* **1991**, *17*, 105−115.
(41) Desimoni, E.; Casella, G. I.; Morone, A.; Salvi, A. M. *Surf. Interface Anal.* **1990**, *16*, 627−634.
(42) Wagner, C. D.; Riggs, W. M.; Davis, C. E.; Moulder, J. F.; Muilenberg, G. E. *Handbook of X-ray Photoelectron Spectroscopy*; Perkin-Elmer Corporation: Eden Prairie, MN, 1979.
(43) *NIST X-ray Photoelectron Spectroscopy Database*; Wagner, C. D., Bickham, D. M., Eds.; Standard Reference Data, National Institute of Standards and Technology: Gaithersburg, MD.
(44) Parmingiani, F.; Pacchioni, G.; Illas, F.; Bagus, P. S. Jr. *Electron Spectrosc. and Relat. Phenom.* **1992**, *59*, 255−269.

of metal/carbon for zinc-containing activated carbon is 0.53 (3.0/5.6), which may be related to the heterogeneity of the surface. These metal/carbon ratios are consistent with surface metal carbonates and carboxylates.

Even though considerable results for carbon fibers and polymers of the O 1s region after plasma treatment exist,[36,40] chemical reactivity of carbon fibers after removing oxygen-containing functional groups can lead to complicated spectra.[41,42] The O 1s region has not been used for separating different functional groups here because this transition does not show readily identifiable separate components such as shoulders. The peaks centered at 532.25 eV for Cu-impregnated carbon, 532.86 eV for Mo impregnated carbon, and 533.17 eV for zinc-containing carbon are mainly due to oxygen on the surface. However, significant signals at binding energies of about 531 eV might be due to metal carbonates and metal carboxylates.[37,38,43,44]

XPS data for similar systems have been used to obtain detailed information about the chemical state of metals impregnated on activated carbon.[45,46] In the other research,[25,26] the binding energies of the Cu $2p_{3/2}$ transitions on copper-impregnated samples were reported as 934 and 933.4 eV and copper compounds were interpreted as cupric oxides. A binding energy of Cu $2p_{3/2}$ of 935.05 eV was observed in our study.

The binding energies of $CuCO_3$ and $Cu(OH)_2$ are 935 eV[44] and 934.8 ± 0.3 eV[43,44,46] and 933.6 ± 0.1 eV.[44,46] The binding energy of Cu $2p_{3/2}$ on Cu-impregnated activated carbon, 935.05 eV, is different from CuO and rather close to that of $CuCO_3$ or $Cu(OH)_2$. No visual shoulder in the peaks of Cu $2p_{3/2}$ and $2p_{5/2}$ to the lower binding energy side was seen. The full width at half-maximum (fwhm) values of Cu $2p_{5/2}$ in copper impregnated activated carbon and $CuCO_3$ collected at the same instrument parameters were 4.55 and 3.45 eV. Both peaks are broader on the higher binding energy side than on the lower binding energy side, which suggests that Cu_2O is not present. In the case of Zn-containing carbon, the binding energy of Zn $2p_{3/2}$ is 1023.53 eV, which is different from $Zn(OH)_2$ and ZnO, 1022.7 ± 0.1[44,46] and 1021.8 ± 0.3 eV.[44,46] From combined XPS and SAM analyses, it can be concluded that some of the metals on the samples very likely exist as metal carbonates and metal carboxylates.

Our results indicate that the presence of metal carbonates and carboxylates are unique to single metal adsorbents. Multiple metal adsorbents with similar preparatory treatments appear as metal oxides.

Overview. TGA and BET results show that some of the mesopores are blocked after metal impregnation. The presence of hydrogen bonded O−H, alkane and alkene C−H, conjugated C═O, C═C, C−O, as well as C−O−C−O−C bonding is observed by diffuse reflectance IR. After metal impregnation new peaks at 1379 cm^{-1} are present and indicative of a metal carbonate or carboxylate. Two peaks in the 1140−1100 cm^{-1} region merge to one peak at 1108 cm^{-1} (Figure 3B,C), which is ascribed to ring opening of a lactone moiety and cyclic ether C−O bond breakage during metal impregnation. Grinding activated carbon results in the dilution of the functional groups on the surface of the granules.

The concentrations of metals and oxygen appear higher on the surface than the interior of the granules from SAM data. The oxygen/metal ratios from SAM analysis are higher than those by XPS. This difference is related to decomposition of metal carbonates to metal oxides by the electron beam during the SAM analysis. Such sample damage has been verified by continuous SAM analysis of metal carbonates. Oxygen/metal ratios are close to 1.08 for $ZnCO_3$ after 5 h of SAM analysis and 1.33 for $CuCO_3$ after 6 h of analysis.

The amount of carbon due to carbonates and carboxylates is calculated based on the binding energies of C 1s peaks after deconvolution of the C 1s region. From the binding energy of Cu $2p_{3/2}$, $CuCO_3$ and $Cu(OH)_2$ are believed to exist on the granules. Binding energies for Zn for Zn-containing activated carbons are different from those of ZnO or $Zn(OH)_2$. There is no significant difference among the IR spectra for Cu- and Mo-impregnated carbons; however, XPS and SAM analyses show the presence of different carbonate and hydroxide species.

Conclusions

There is a small amount of reduction in surface area with metal impregnation due to covering of some of the surface or filling of some mesopores on the basis of N_2 adsorption data. However, adsorption isotherms with N_2 gas for all single-metal-loaded samples and plain activated carbon were the same showing typical type I isotherms.

After grinding the activated carbon granules, the surface hydrophilic functional groups are less abundant with respect to interior polyaromatic structures on the basis of FTIR data. Interior analyses of the granules by SAM also show less oxygen content. From the results of DRIFT, SAM, and XPS studies, external sites of the granules have more hydrophilic functional groups containing oxygen than internal sites, but the sulfur content is fairly evenly distributed throughout the granule and exists in carbonaceous environments even after metal impregnation.

The use of a sensitive detector (MCT) and long scans in the mid-IR region have led to the observation of new functional groups on activated and metal-activated carbon samples. This may allow further in-depth functional group studies on surfaces of activated carbons-containing metals.

Metal contents in the samples from ICP-AES appear to be lower than original loadings. Some of the Cu moieties may exist as forms of $CuCO_3$ and $Cu(OH)_2$. Zn probably exists as $ZnCO_3$. Mo is distributed through the granules, but not evenly dispersed in oxidized forms. Cu and Zn exist primarily on the surface rather than in the interior.

Acknowledgment. The authors would like to thank the US ERDEC for support of this research, Dr. William S. Willis for help in collecting XPS data as well as helpful discussions, and Donald F. Hobro and Jonathan Martin at Environmental Research Institute of the University of Connecticut for elemental analyses. We thank Dr. David Tevault for helpful discussions.

CM9602712

(45) Deroubaix, G.; Marcus, P. *Surf. Interface Anal.* **1992**, *18*, 39−46.

(46) Wagner, C. D.; Zatko, D. A.; Raymond, R. H. *Anal. Chem.* **1980**, *52*, 1445−1451.